Study on the Structure and Properties of Conductive Silicone Rubber Filled with Nickel-Coated Graphite

Hua Zou,[1] Liqun Zhang,[1,2] Ming Tian,[1] Sizhu Wu,[2] Suhe Zhao[2]

[1]*The Key Laboratory for Nano Materials, Ministry of Education, Beijing University of Chemical Technology, Beijing 100029, China*
[2]*Beijing City Key Laboratory of Preparation and Processing of Novel Polymer Materials, Beijing University of Chemical Technology, Beijing 100029, China*

Received 10 April 2008; accepted 18 December 2008
DOI 10.1002/app.29901
Published online 26 October 2009 in Wiley InterScience (www.interscience.wiley.com).

ABSTRACT: In this study, the conductive silicone rubber composites filled with nickel-coated graphite (NCG) have been prepared, and their morphology structure, electrical conductivity, electromagnetic interference shielding efficiency (EMI SE), and mechanical properties have been investigated with reference to the NCG filler loading. The mechanical strength of NCG particle was poor that it can be easily ground into smaller particle during the mixing process if the shear force during mixing is large enough. The electrical conductivity of the composites existed an obvious threshold value with the variation of the loading amount of the conductive filler. EMI SE of the composites increases with the decrease of the volume electrical resistivity. The Payne effect can be used to characterize the intensity of the three-dimensional conductive network structure in silicone rubber matrix, and the difference of storage modulus in the low and high shear strain has good linear correlation with the electrical conductivity. So, the electrical conductivity and EMI SE can be estimated by means of the difference of storage modulus obtained from rubber process analysis test.
 J Appl Polym Sci 115: 2710–2717, 2010

Key words: polysiloxanes; rubber; morphology; electrical conductivity; shielding efficiency

INTRODUCTION

Electrically conductive rubbers have drawn considerable interest for a long time. Recent interest has been growing because of their application in newer areas such as electronic equipment, pressure sensitive switches, and other important strategic materials such as electromagnetic interference (EMI) shielding, apart from the conventional application of semiconducting materials for dissipation of static electricity.[1] It is well known that insulating rubber can be made conductive through incorporation of conductive filler. Various rubbers have been used for preparation of such composites, for example natural rubber,[1] styrene–butadiene rubber,[2–4] nitrile rubber,[5] ethylene–propylene–diene rubber,[6,7] silicone rubber,[8–11] or rubber–rubber blends, etc.[12–14] Common conductive fillers include electrically conductive carbon black,[2–5,7,12,13] graphite, carbon fiber,[1,13–16] carbon nanotube,[17] pure metal,[18] metal-coated inorganic particles, and metal powders.[19–22] Among different types of conductive fillers, carbon black is the most widely used materials for rubber matrix. Not only it provides a high degree of conductivity but also imparts good reinforcement to the rubber matrix. However, in many applications, high conductivity is the main requirement and the mechanical properties may be a secondary consideration. To achieve the higher conductivity at lower loading, pure metal powder such as silver,[18] nickel, and aurum or metal-coated material such as silver-coated,[22] nickel-coated filler may be a better choice than conductive carbon black. Nickel-coated materials such as nickel-coated mica, carbon fiber, and PET fiber, which combine good performance, low cost, and good stability, have drawn considerable interest in the past decades.[23–25] But up to now, study on the electrically conductive silicone rubbers composite filled with nickel-coated graphite (NCG) has not been reported from reference. In this study, the electrical conductivity and EMI shielding efficiency (SE) of silicone rubber composites filled with NCG have been investigated. The network structure of conductive filler in rubber matrix has been studied in detail by means of RPA2000 analyzer with a view to understand the mechanism of conductivity. The mechanical properties have also been measured to characterize the suitability of these composites in other practical application as a reference to further development of superior electrically conductive rubber composites for EMI shielding.

Correspondence to: S. Zhao (zhaosh@mail.buct.edu.cn).

TABLE I
Formulation of Nickel-Coated Graphite Filler Silicone Rubber (phr[a])

	N0	N20	N40	N60	N80	N100	N120	N140	N160	N180	N200
VMQ	100	100	100	100	100	100	100	100	100	100	100
NCG	0	20	40	60	80	100	120	140	160	180	200
A151	0	0.6	1.2	1.8	2.4	3	3.6	4.2	4.8	5.4	6
DCBP	2	2	2	2	2	2	2	2	2	2	2
Vol % of NCG	0	4.7	9.0	12.9	16	19.8	22.9	25.7	28.3	30.8	33.1

[a] phr is the abbreviation of parts per hundred of base polymer, which is the weight parts per 100 weight parts of rubber in this study.

EXPERIMENTAL

Material

Methyl vinyl silicone rubber masterbatch (VMQ, Grade KE931-U, silica-containing) with the density 1.07 g/cm^3 was manufactured by Shin-Etsu Chemical Co., Tokyo, Japan. Nickel-coated graphite with a weight composition of 60% nickel and 40% graphite, used as the electrical conductive filler, was supplied by Novamet Specialty Products Corporation, Wyckoff, NJ. The particle size range was 60–140 μm with an average particle size of 100 μm. The true particle density and apparent density of NCG powder was 4.3 and 1.45 g/cm^3, respectively. Vulcanizing agent, bis (2,4-dichlorobenzoyl) peroxide (DCBP), grade Enox® DCBP, was purchased from Qiangsheng Chemical Engineering Company, Changshu City, Jiangsu Province, China. The coupling agent vinyltriethoxysilane (A151) was obtained from Nanjing Shuguang Chemical Group Co., Nanjing City, Jiangsu Province, China.

Sample preparation of VMQ/NCG composites

The compound formulations were given in Table I. NCG powder, A151, and DCBP were mixed with silicone rubber at 25°C, using a two-roll mill. The compounds were then cured at 112°C for 10 min in an electrically heated press with the pressure of 10 MPa. The 2-mm-thick cured sheets were then kept at 200°C for 2 h for postcure and then kept at room temperature for 24 h before testing.

Characterization

The morphology of NCG powder and NCG/VMQ composites was observed using a XL-30 environmental scanning electron microscopy (ESEM) with an acceleration voltage of 15 kV, manufactured by Philips-FEI Company, Eindhoven, Netherlands. VMQ/NCG composites were immersed into liquid nitrogen to get the brittle fractured surface and then coated with gold–palladium film for further observation. The NCG powder was dispersed in sample platform and coated with gold–palladium film.

The volume resistivity (ohm cm) of the compositions with a high resistivity was tested using a high-resistance meter (Model ZC36, manufactured by Shanghai Shenguang Instrument Co., Shanghai City, China). For composites with low resistance, the volume resistivity was obtained by a four-probe technique using a QJ84 (Shanghai Zhengyang Instrument Plant, Shanghai City, China) microohm meter according to ASTM D991. Before tested, the aforementioned vulcanized rubber sheets were cut into 10 mm × 100 mm × 2 mm strips, washed with alcohol, and kept to dry completely. The volume resistivity data used were the average results of the five samples.

The EMI SE of VMQ/NCG composites was measured by the network analyzer (Model HP8752A, Agilent Technologies, Santa Clara, CA) using the coaxial cable line test method according to ASTM ES-7-83. The specimens were cut into disc with a diameter of 115 mm. The SE value was obtained by measuring the attenuation or reduction of the electromagnetic wave with or without the shield sample in the frequency of 30, 70, 100, 200, 300, 500, 800, 1000, 1200, 1500 MHz, respectively. The SE can be calculated and expressed in decibels (dB) by using the following eq. (1):

$$\mathrm{SE} = 10\ \mathrm{Log}\left(\frac{P_1}{P_0}\right) = 20\ \mathrm{Log}\left(\frac{E_1}{E_0}\right) = 20\ \mathrm{Log}\left(\frac{H_1}{H_0}\right) \quad (1)$$

where P_0, E_0, and H_0 are energy field strength, electric field strength, and magnetic field strength of the transmitted wave, respectively. The P_1, E_1, and H_1 are the above corresponding properties of the incident wave.

The network structure of conductive filler in VMQ/NCG composites was characterized by a RPA2000 rubber processing analyzer from Alpha Technologies Co., Akron, OH. The strain dependence of the dynamic modulus G' of the mixing rubber was determined by increasing the strain amplitude from 0.7 to 399.95% at a constant temperature of 60°C and a frequency of 1 Hz. As for vulcanized conductive rubber, the strain dependence of the dynamic modulus G' was measured at 60°C and 1 Hz as a function of strain amplitude from 0.28 to 39.76%.

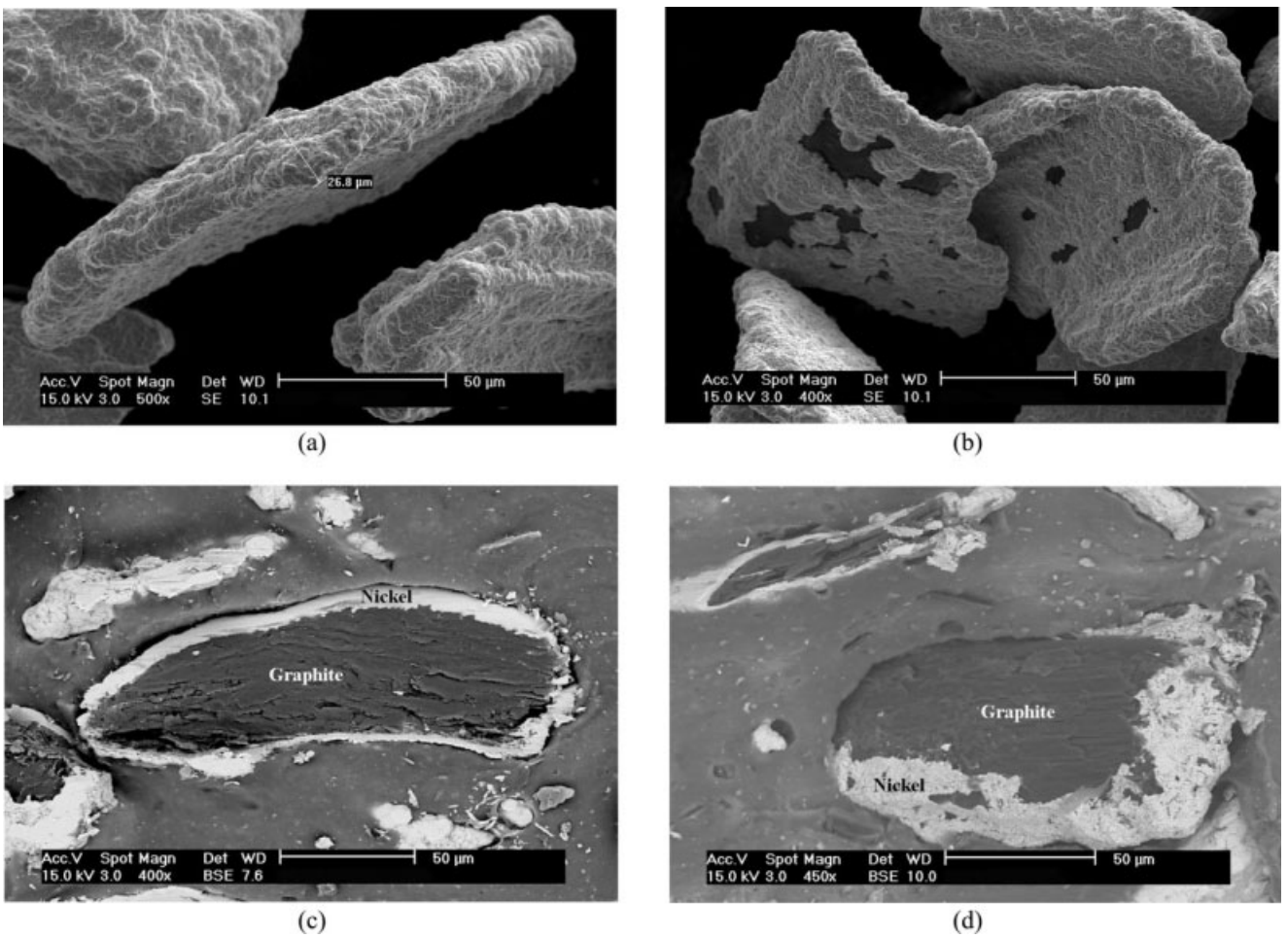

Figure 1 ESEM micrographs of (a) and (b) nickel-coated graphite; (c) and (d) tensile fractured surface of conductive polymer filled with 200 phr NCG.

Tensile properties were measured using a Universal Testing Machine CMT4104 (Shenzhen SANS Group Company, Shenzhen City, Guangdong Province, China) with the crosshead speed of 500 mm/min based on the standard of ASTM-D 751. Five specimens were tested and the average value was reported.

RESULTS AND DISCUSSION

Morphology structure of NCG powder

The microstructure of the NCG powder observed by the ESEMs was shown in Figure 1. It can be seen that the NCG particles were flake-shaped with an average thickness of 20–30 μm. The core of the electrically conductive filler was loose expanded graphite and not completely encapsulated by the nickel outer skin. The nickel coating deposited on the graphite core has a coarse surface. Figure 1(c,d) showed the tensile fractured surface of conductive polymer filled with 200 phr NCG. It can be seen that there are some small nickel particles peeled from NCG particle, and some NCG particles have been fractured, naked, or ground into small particles in the rubber matrix, indicating that the NCG particle has poor mechanical strength. Considering the strength of the rubber matrix is low, it is thought that the breakage of the NCG particles occurred during the blending process. So, in the blending process, the shear force provided by mixer should be controlled in an appropriate range. Too large shear force would peel the partial nickel skin from the graphite core or the total fracture of the conductive particle, whereas too small shear force would not disperse uniformly the conductive particle into the rubber matrix.

Electrically conductivity and mechanical properties of NCG/VMQ composites

In general, there are two kinds of possible electrical paths in conductive polymer filled with conductive filler.[26–28] The first and probably the most efficient way involves filler–filler contact. The continuum of the conductive filler particles thus provides the conductive bands for movement of the electrical charge. In the second, the electronic conduction process

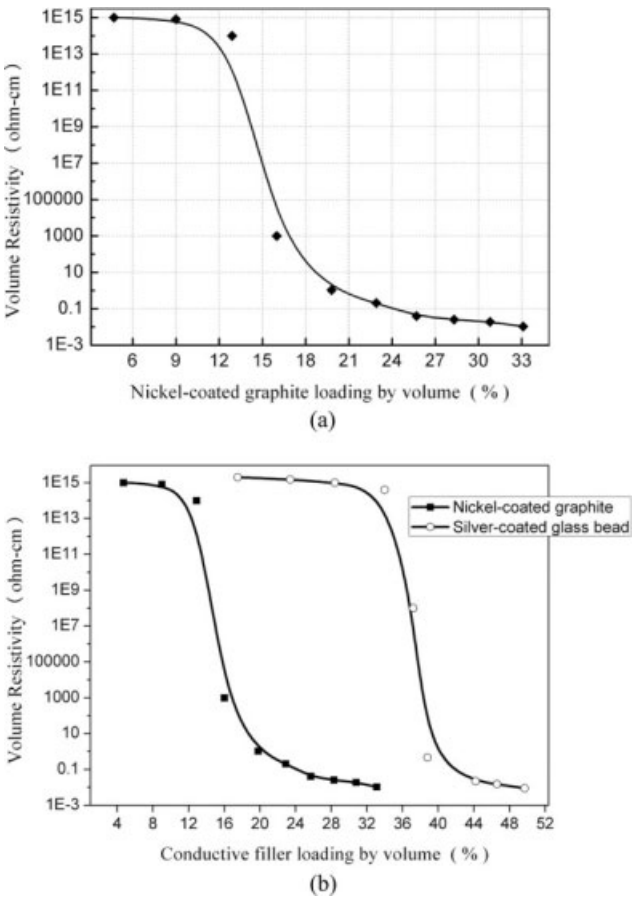

Figure 2 The relationship of volume resistivity and filler loading by volume (a) nickel-coated graphite and (b) nickel-coated graphite vs. silver-coated glass bead.

across the gaps and/or the insulating matrix rubber layer that separates the conductive filler particles from each other, representing electrical potential barriers. This is the so-called tunneling effect, whereby electrons jump from one side of a potential gap to the other. So, the conductivity and the volume content of the filler is the most important factor to the electrical conductive composites. Equation (2) can be used to convert between weight percent and volume percent loading for any combination of filler and polymer.

$$\text{Vol.}(\%) = \frac{W_F}{W_p \times (\frac{d_F}{d_P}) + W_F} \times 100\% \qquad (2)$$

where W_F, W_P are the respective filler and polymer weight, and d_F, d_P are the respective true density of conductive filler and polymer matrix, respectively.

The volume fraction of the conductive filler in the silicone rubber matrix was calculated according to the eq. (2), which the plot of volume resistivity as a function of volume fraction was given in Figure 2(a). It can be seen that the composites become electrically conductive as the volume fraction of the NCG exceeds a critical value. Under 12.9 vol %, the volume resistivity of the composites was as high as 10^{14} ohm cm and behaves insulative. Once the volume fraction exceeds 12.9%, the volume resistivity of the composites decreases rapidly from 10^{14} (12.9 vol %) to 10^3 ohm cm (16 vol %). Above the 16 vol %, the decrease extent of volume resistivity becomes slow. It can be seen clearly from Figure 2(a) that the percolation threshold concentration of the NCG-filled silicone rubber composites from insulator to conductor was between 12.9 and 16 vol %. The reason might be when the conductive filler content increases at first, the filler particle becomes close enough to allow the electrons to hop across gaps among the conductive filler particles. Once the percolation threshold concentration was reached, the integrated catenulate conductive path was formed in the rubber matrix and the electrons can be transferred easily from one end to the other end of the conductive chain, and thus the composites become conductive. Above the percolation threshold concentration, when the filler content further increases, more and more conductive paths were formed and ultimately the three-dimensional conductive network come into being in the silicone rubber matrix.

In former study, the percolation threshold concentration of conductive filler existed in the conductive silicone rubber filled by silver-coated glass bead was also observed.[29] Figure 2(b) showed the relationship between volume resistivity and filler loading by volume of silver-coated glass bead-filled and NCG-filled silicone rubber. It can be seen that the percolation threshold concentration has a great difference between NCG and silver-coated glass bead, about 16 and 38 vol %, respectively, which might be the differences in three-dimensional shape.[30] Compared with the spherical silver-coated glass bead, the flake-shaped NCG particles were easier to contact each other to form conductive path because of high aspect ratio, and the contact area of flake-shaped particles was larger than that of spherical particles.

TABLE II
Mechanical Properties of VMQ/NCG Blends

Compound	Stress at 100% elongation (MPa)	Tensile strength (MPa)	Elongation at break (%)	Shore A Hardness
N0	1.03	4.56 ± 0.07	475 ± 6	30
N60	1.38	2.90 ± 0.03	240 ± 5	42
N80	1.66	3.12 ± 0.08	219 ± 7	49
N100	1.78	3.24 ± 0.06	205 ± 3	54
N120	2.22	3.53 ± 0.06	200 ± 3	59
N140	2.65	3.62 ± 0.08	172 ± 4	62
N160	2.75	3.68 ± 0.04	162 ± 9	65
N180	3.08	3.78 ± 0.09	149 ± 4	69
N200	3.26	3.87 ± 0.02	142 ± 6	73

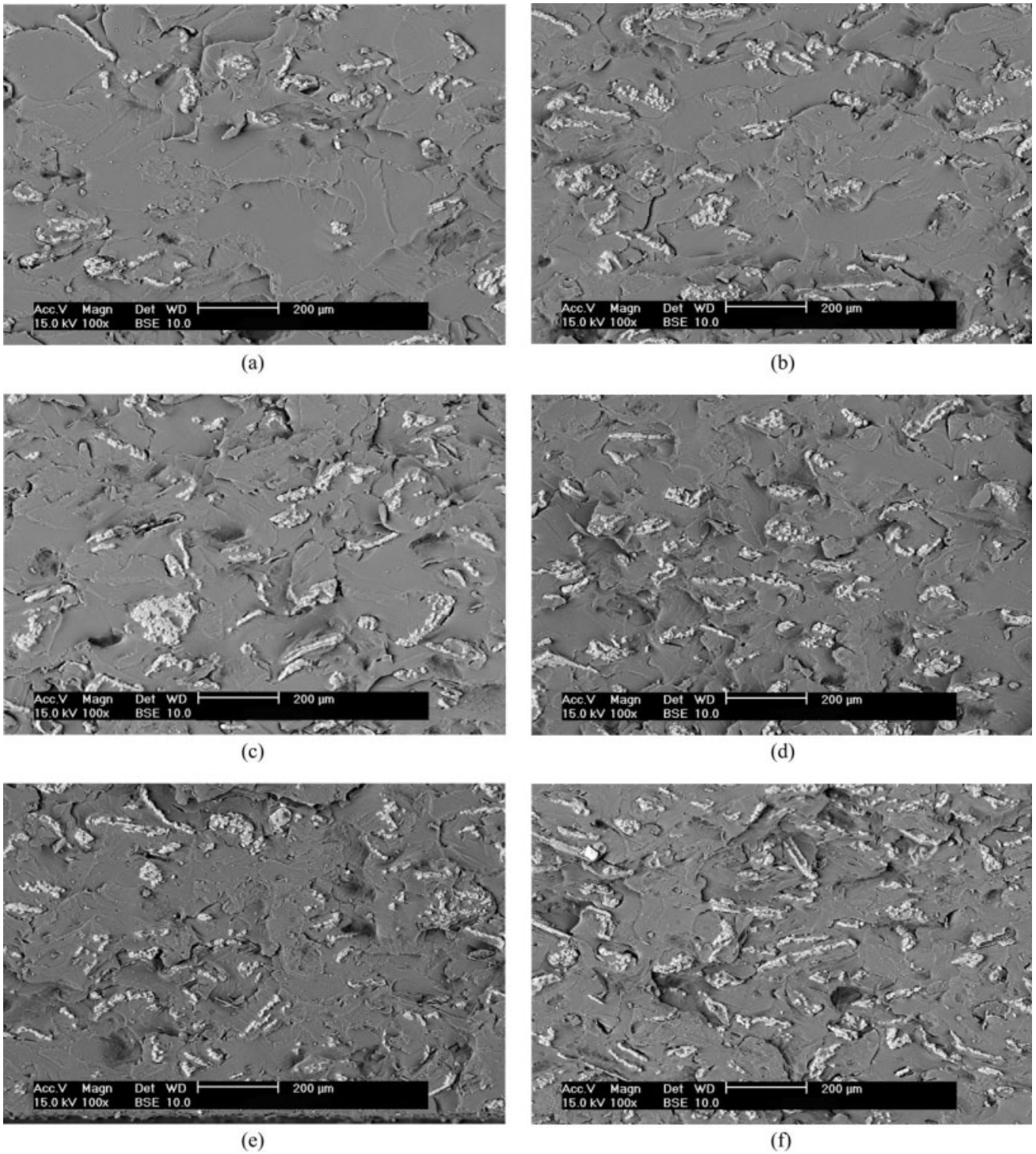

Figure 3 ESEM micrographs of conductive silicone rubber loaded with different amount of NCG. (a) 60 phr, (b) 80 phr, (c) 100 phr, (d) 120 phr, (e) 140 phr, and (f) 160 phr.

The tensile properties of VMQ/NCG blends were summarized in Table II. As seen in the Table II, the stress at 100% elongation and shore A hardness increased with the increase of loading amount of the NCG powder, and the elongation at break decreased with the increase of loading amount of the NCG filler. The tensile strength first dropped drastically from 4.56 to 2.90 MPa, and then showed a slightly increase from 2.90 to 3.87 MPa with the increase of NCG filler from 60 to 200 phr. The phenomena can be explained as following: The NCG-unfilled composites, namely the silica-containing rubber masterbatch KE-931U, showed high tensile strength because of the reinforcing action of silica. When the

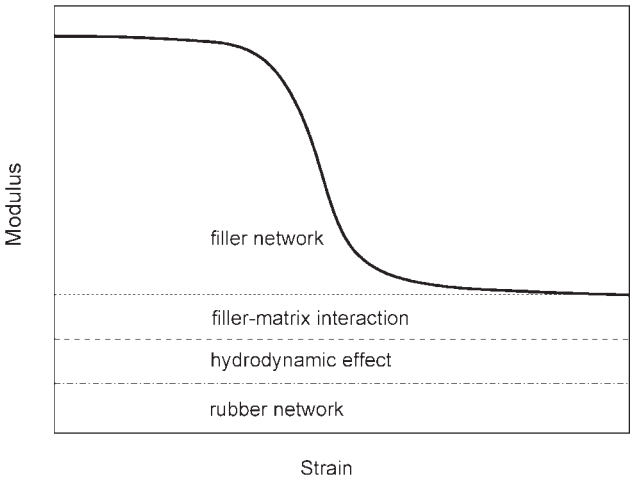

Figure 4 Modulus contributions as a function of strain.

NCG particles were added to VMQ rubber, on the one hand, the tensile strength of the composites decreased sharply owing to the nonreinforcing effect of micron-scale filler. On the other hand, because of the high aspect ratio of NCG particles, the conductive filler showed orientation distribution in the VMQ rubber to a large extent, as shown in Figure 3. According to the interfacial stress transfer mechanism,[31,32] the applied load on the low modulus VMQ rubber can be transferred onto the high modulus NCG particle through the interface between filler and rubber matrix. The NCG particle restricted the deformation of the VMQ rubber and then heightened the tensile strength of the composites. The synthetic results of nonreinforcing effect and interfacial stress transfer effect led to the decrease of elongation at break and slight increase of strength with an increase of NCG loading. It is worth to point out that the slight increase of the tensile strength is very important for the practical applications, because the disadvantage of the high conductive rubber is low mechanical strength.

Microstructure of NCG/VMQ composites and network structure of conductive filler in rubber matrix

Figure 3 showed the SEM micrograph of silicone rubber composites filled with NCG with different loading amounts. It can be seen that in the composites filled with 60 phr NCG, the NCG powders were isolated from each other, so the composite was electrically insulative. When the loading amount was elevated to 80 phr, some local filler–filler contacts formed, but on the whole, there was no entire conductive path in the silicone rubber matrix. When more conductive filler was added to the rubber, more and more filler–filler contacts came into being and ultimately, some conductive paths engendered in the rubber matrix with the conterminous contacts with each other, thus the composites convert from insulator to conductor. From Figure 3, it can also be seen that the conductive filler was dispersed uniform in the silicone rubber matrix and showed orientation distribution to a large extent. Moreover, it can be observed that some NCG particles have separated from the rubber matrix to form some holes in the fractured surfaces. But most of NCG particles stayed in the rubber matrix, which indicated a good interface bonding between the conductive filler and the silicone rubber matrix by means of the couple agent A151.

In the early study, it is found that carbon black-filled rubber showed a typical nonlinear viscoelastic behavior. At strains of about 1%, a significant decrease of storage modulus occurred from the zero-strain value G'_0 to a high amplitude plateau value G'_∞ connected with the appearance of a loss modulus G'' maximum. This effect was described by

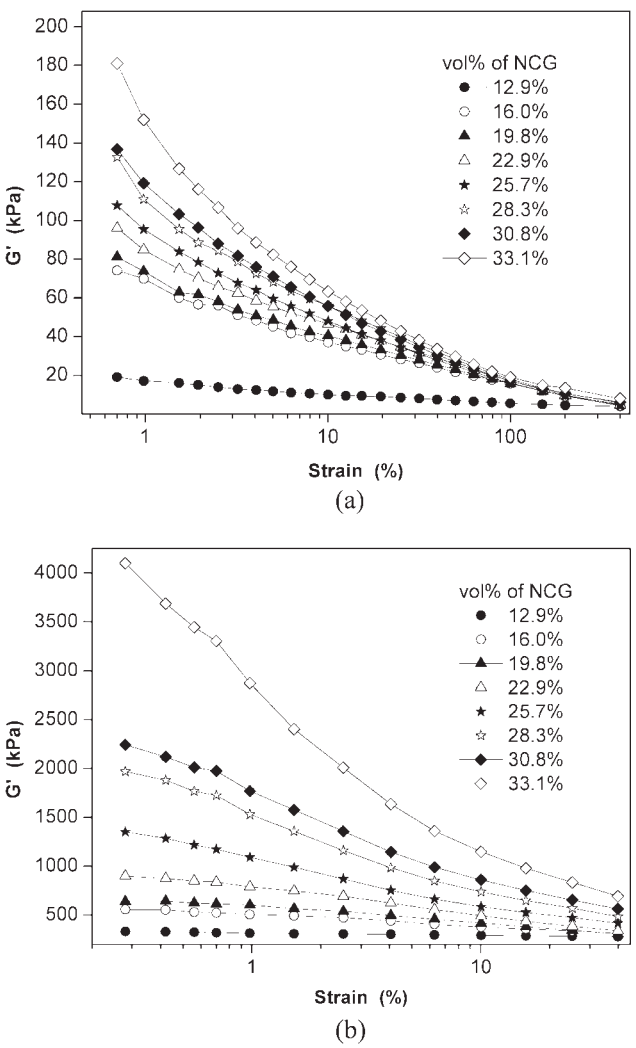

Figure 5 Relationship of storage modulus and strain. (a) Mixing rubber and (b) vulcanization rubber.

Payne in the 1960s.[33–35] It was interpreted as the result of breakage and reforming of physical bonds between the filler aggregates. These bonds were assumed to build filler agglomerates and, above a certain threshold, a rigid filler network forms within the rubber matrix. A general schematic illustration of dynamic modulus[36] was given in Figure 4. The modulus was composed from the following parts, which did not depend on the strain: the pure rubber network, the hydrodynamic effect, specific filler–matrix interactions, and in addition, a strain-dependent part caused by the filler network. So, the difference value of storage modulus in the initiative and final strain can be used to characterize the network structure strength of filler in rubber matrix.

Figure 5 was presented to show the typical results for the Payne effect of the mixing rubber and vulcanized rubber. From these figures, it can be seen that both the mixture rubber and the vulcanized rubber showed strain amplitude dependencies of the viscoelastic properties, and the Payne effect both in the mixing rubber and in the vulcanization increased gradually with increasing the loading amount of the conductive filler. Moreover, as for the same loading amount, for example 200 phr, the difference value of storage modulus $\Delta G'$ ($=G'_{\mathrm{Onset}} - G'_{\mathrm{Endset}}$) in the vulcanization sample was larger than in the mixture rubber, showing stronger Payne effect in vulcanization rubber.

Because the $\Delta G'$ value can be used to character the network structure strength of filler in rubber matrix, and the three-dimensional network structure of conductive filler was the most important factor to form the electrical conductive composites, therefore $\Delta G'$ value can be employed to characterize the electrically conductivity of the composites. Figure 6 showed the plots of $\Delta G'$ ($=G'_{\mathrm{Onset}} - G'_{\mathrm{Endset}}$), the conductivity of the vulcanized rubber, and the volume fraction of NCG. It can be seen that the $\Delta G'$ value and the volume conductivity both rise with the increase of the volume content of the conductive filler, and they follow the same uptrend.

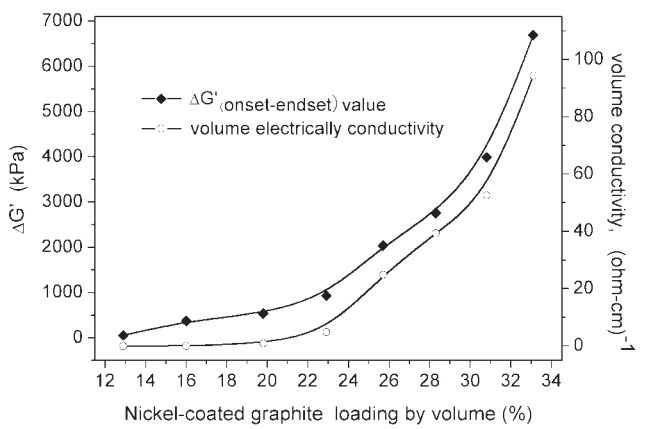

Figure 6 Plots of $\Delta G'$ value, volume conductivity, and the volume content of nickel-coated graphite in rubber matrix.

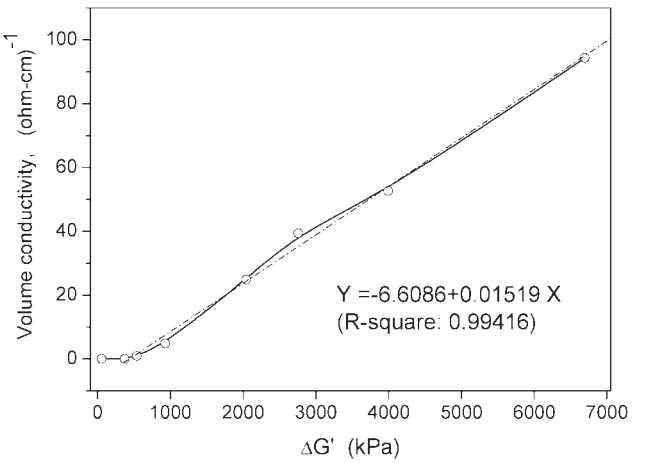

Figure 7 Linear relationship between $\Delta G'$ value and volume conductivity.

Figure 7 showed the relationship between $\Delta G'$ and volume conductivity of cured rubber. By means of linearization analysis, it was found that there is a good linear relationship between $\Delta G'$ and conductivity in the conductive zone, which can be described with the following equation:

$$Y = -6.6086 + 0.01519X \tag{3}$$

where the correlation coefficient R^2 reached to 0.99416.

EMI shielding efficiency

EMI SE versus frequency plots for the NCG-filled silicone rubber were shown in Figure 8. It can be observed that the EMI SE of the composites increased continuously with the increase in filler

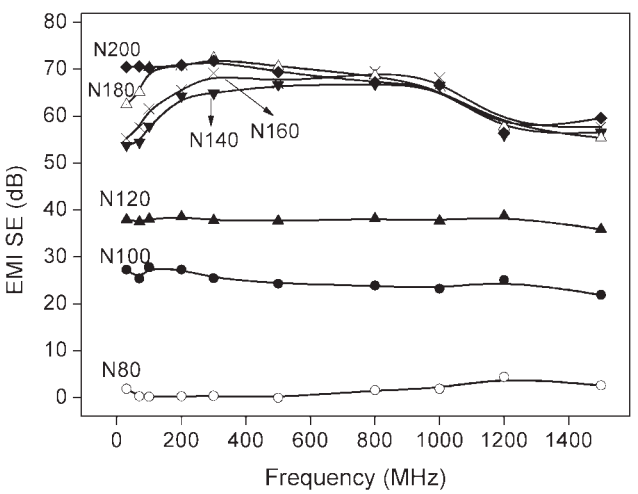

Figure 8 Shielding efficiency of nickel-coated graphite-filled silicone rubber composites.

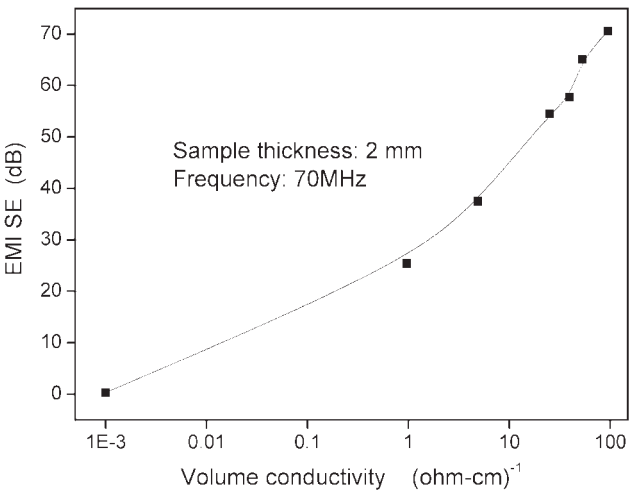

Figure 9 Relationship between EMI SE and volume conductivity of conductive rubber.

loading. The composite filled with 80 phr NCG had only SE around 0–5 dB, showing rather poor shielding property. The composites that contain 100 and 120 phr conductive filler had the SE value of 20–30 and 40 dB, respectively, suggesting that about 90 and 99% of electromagnetic wave can be attenuated, which can satisfy the EMI shielding demand in the most commercial field. When the loading amount of conductive filler rose to 140 phr and more, the SE value increased gradually and reached 60–70 dB, denoting above 99.9% of the electromagnetic wave can be attenuated.

The relationship between EMI SE and the volume resistivity of the vulcanized composites was shown in Figure 9. It can be observed that SE increased gradually with the drop of volume resistivity, which implied that the EMI SE can be estimated by the volume resistivity of the composite materials.

CONCLUSIONS

In this work, the effect of NCG conductive filler loading on the morphology structure, electrical conductivity, mechanical properties, and EMI shielding properties of VMQ/NCG composites has been investigated. It was found that NCG particles had poor mechanical strength that it can be ground into smaller particle during the blending process if the shear force was too large. The electrical conductivity of VMQ/NCG composites increased with the increase of NCG filler loading, and the threshold value of VMQ/NCG was lower than that of VMQ composites filled with silver-coated glass bead. With the increase of NCG filler loading, elongation at break decreased, and the tensile strength went down first and then up because of the synthetical influence of nonreinforcing effect and interfacial stress transfer effect. EMI SE of the composites increased with the decrease of the volume electrical resistivity. The difference of storage modulus in the low and high shear strain had good linear correlation with the electrical conductivity, so electrical conductivity and EMI SE can be estimated by means of the difference of storage modulus obtained from RPA test.

References

1. Das, N. C.; Khastgir, D.; Chaki, T. K.; Chakraborty, A. Compos A 2000, 31, 1069.
2. Nasr, G. M. Polym Test 1996, 15, 585.
3. Mohanraj, G. T.; Chaki, T. K.; Chakraborty, A.; Khastgir, D. Polym Eng Sci 2006, 46, 1342.
4. Mohanraj, G. T.; Chaki, T. K.; Chakraborty, A.; Khastgir, D. J Appl Polym Sci 2004, 92, 2179.
5. Pramanik, P. K.; Khastgir, D.; Saha, T. N. Plast Rubber Compos Process Appl 1992, 17, 179.
6. Mauro, A. S.; Olacir, A. A.; Roselena, F.; Mirabel, C. R.; Macro-A, D. P. Synth Met 2006, 156, 1249.
7. Premamoy, G.; Amit, C. Eur Polym J 2000, 36, 1043.
8. Sau, K. P.; Khastgir, D.; Chaki, T. K. Die Angew Makromol Chem 1998, 258, 11.
9. Wang, L. H.; Ding, T. H.; Wang, P. Sens Actuators A 2007, 135, 587.
10. Duan, Y. P.; Liu, S. H.; Guan, H. T. Sci Technol Adv Mater 2005, 6, 513.
11. Princy, K. G.; Joseph, R.; Kartha, C. S. J Appl Polym Sci 1998, 69, 1043.
12. Das, N. C.; Chaki, T. K.; Khastgir, D. Carbon 2002, 40, 807.
13. Sau, K. P.; Chaki, T. K.; Khastgir, D. J Mater Sci 1997, 32, 5717.
14. Sau, K. P.; Chaki, T. K.; Khastgir, D. Polymer 1998, 39, 6461.
15. Jana, P. B.; Chaudhuri, S.; Pai, A. K.; De, S. K. Polym Eng Sci 1992, 32, 448.
16. Jana, P. B.; Mallick, A. K.; De, S. K. J Mater Sci 1993, 28, 2097.
17. Yoong, A. K.; Takuaya, H.; Morinobu, E.; Yasuo, G.; Noriaki, W.; Junji, S. Scr Mater 2006, 54, 31.
18. Lee, H. H.; Chou, K. S.; Shih, Z. W. Int J Adhes Adhes 2005, 25, 437.
19. Joon, J.; Seung, K. R. J Mater Process Technol 2006, 180, 66.
20. Novák, I.; Krapu, I.; Chodák, I. Synth Met 2004, 144, 13.
21. Liang, T. X.; Guo, W. L.; Yan, Y. H.; Tang, C. H. Inter J Adhes Adhes 2007, 03, 006.
22. Walther, J. F. Proceedings of the IEEE National Symposium on Electromagnetic Compatibility; IEEE: Denver, 1989.
23. Kortschot, M. T.; Woodhams, R. T. Polym Compos 1985, 6, 296.
24. Ahmad, M. S.; Zihilif, A. M.; Martuscelli, E.; Ragosta, G.; Scafora, E. Polym Compos 1992, 13, 53.
25. Chiang, W. Y.; Chiang, Y. S. J Appl Polym Sci 1992, 46, 673.
26. Wber, M.; Kamal, M. R. Polym Compos 1997, 18, 711.
27. Ruschau, G. R.; Yoshikawa, S.; Newnham, R. E. J Appl Phys 1992, 72, 953.
28. Medalia, A. I. Rubber Chem Technol 1986, 59, 432.
29. Zhang, J. Y.; Zou, H.; Tian, M.; Shen, L.; Zhang, L. Q.; Qu, X. W. Spec Purpose Rubber Prod (In Chinese) 2007, 28, 19.
30. Lux, F. J Mater Sci 1993, 28, 285.
31. Zhang, L. Q.; Jin, R. G.; Geng, H. P.; Chen, S.; Zhou, Y. H. Acta Mater Compos Sin 1998, 15, 89.
32. Pegormti, A.; Fambfu, L.; Migliaresi, C. Polym Compos 2000, 21, 466.
33. Heinrich, G.; Klüppel, M. Adv Polym Sci 2002, 160, 1.
34. Wang, M. J. Rubber Chem Technol 1998, 73, 520.
35. Drozdov, A. D.; Dorfmann, A. L. Polym Eng Sci 2002, 42, 591.
36. Fröhlich, J.; Niedermeier, W.; Luginsland, H. D. Compos A 2005, 36, 449.